Measurement of the $B^- \to D^0 K^{*-}$ branching fraction

B. Aubert,[1] R. Barate,[1] D. Boutigny,[1] F. Couderc,[1] Y. Karyotakis,[1] J. P. Lees,[1] V. Poireau,[1] V. Tisserand,[1] A. Zghiche,[1] E. Grauges,[2] A. Palano,[3] M. Pappagallo,[3] J. C. Chen,[4] N. D. Qi,[4] G. Rong,[4] P. Wang,[4] Y. S. Zhu,[4] G. Eigen,[5] I. Ofte,[5] B. Stugu,[5] G. S. Abrams,[6] M. Battaglia,[6] D. S. Best,[6] D. N. Brown,[6] J. Button-Shafer,[6] R. N. Cahn,[6] E. Charles,[6] C. T. Day,[6] M. S. Gill,[6] A. V. Gritsan,[6,*] Y. Groysman,[6] R. G. Jacobsen,[6] J. A. Kadyk,[6] L. T. Kerth,[6] Yu. G. Kolomensky,[6] G. Kukartsev,[6] G. Lynch,[6] L. M. Mir,[6] P. J. Oddone,[6] T. J. Orimoto,[6] M. Pripstein,[6] N. A. Roe,[6] M. T. Ronan,[6] W. A. Wenzel,[6] M. Barrett,[7] K. E. Ford,[7] T. J. Harrison,[7] A. J. Hart,[7] C. M. Hawkes,[7] S. E. Morgan,[7] A. T. Watson,[7] M. Fritsch,[8] K. Goetzen,[8] T. Held,[8] H. Koch,[8] B. Lewandowski,[8] M. Pelizaeus,[8] K. Peters,[8] T. Schroeder,[8] M. Steinke,[8] J. T. Boyd,[9] J. P. Burke,[9] W. N. Cottingham,[9] D. Walker,[9] T. Cuhadar-Donszelmann,[10] B. G. Fulsom,[10] C. Hearty,[10] N. S. Knecht,[10] T. S. Mattison,[10] J. A. McKenna,[10] A. Khan,[11] P. Kyberd,[11] M. Saleem,[11] L. Teodorescu,[11] V. E. Blinov,[12] A. D. Bukin,[12] A. Buzykaev,[12] V. P. Druzhinin,[12] V. B. Golubev,[12] A. P. Onuchin,[12] S. I. Serednyakov,[12] Yu. I. Skovpen,[12] E. P. Solodov,[12] K. Yu Todyshev,[12] M. Bondioli,[13] M. Bruinsma,[13] M. Chao,[13] S. Curry,[13] I. Eschrich,[13] D. Kirkby,[13] A. J. Lankford,[13] P. Lund,[13] M. Mandelkern,[13] R. K. Mommsen,[13] W. Roethel,[13] D. P. Stoker,[13] S. Abachi,[14] C. Buchanan,[14] S. D. Foulkes,[15] J. W. Gary,[15] O. Long,[15] B. C. Shen,[15] K. Wang,[15] L. Zhang,[15] D. del Re,[16] H. K. Hadavand,[16] E. J. Hill,[16] H. P. Paar,[16] S. Rahatlou,[16] V. Sharma,[16] J. W. Berryhill,[17] C. Campagnari,[17] A. Cunha,[17] B. Dahmes,[17] T. M. Hong,[17] J. D. Richman,[17] T. W. Beck,[18] A. M. Eisner,[18] C. J. Flacco,[18] C. A. Heusch,[18] J. Kroseberg,[18] W. S. Lockman,[18] G. Nesom,[18] T. Schalk,[18] B. A. Schumm,[18] A. Seiden,[18] P. Spradlin,[18] D. C. Williams,[18] M. G. Wilson,[18] J. Albert,[19] E. Chen,[19] G. P. Dubois-Felsmann,[19] A. Dvoretskii,[19] D. G. Hitlin,[19] I. Narsky,[19] T. Piatenko,[19] F. C. Porter,[19] A. Ryd,[19] A. Samuel,[19] R. Andreassen,[20] G. Mancinelli,[20] B. T. Meadows,[20] M. D. Sokoloff,[20] F. Blanc,[21] P. C. Bloom,[21] S. Chen,[21] W. T. Ford,[21] J. F. Hirschauer,[21] A. Kreisel,[21] U. Nauenberg,[21] A. Olivas,[21] W. O. Ruddick,[21] J. G. Smith,[21] K. A. Ulmer,[21] S. R. Wagner,[21] J. Zhang,[21] A. Chen,[22] E. A. Eckhart,[22] A. Soffer,[22] W. H. Toki,[22] R. J. Wilson,[22] F. Winklmeier,[22] Q. Zeng,[22] D. D. Altenburg,[23] E. Feltresi,[23] A. Hauke,[23] H. Jasper,[23] B. Spaan,[23] T. Brandt,[24] V. Klose,[24] H. M. Lacker,[24] R. Nogowski,[24] A. Petzold,[24] J. Schubert,[24] K. R. Schubert,[24] R. Schwierz,[24] J. E. Sundermann,[24] A. Volk,[24] D. Bernard,[25] G. R. Bonneaud,[25] P. Grenier,[25,†] E. Latour,[25] Ch. Thiebaux,[25] M. Verderi,[25] D. J. Bard,[26] P. J. Clark,[26] W. Gradl,[26] F. Muheim,[26] S. Playfer,[26] Y. Xie,[26] M. Andreotti,[27] D. Bettoni,[27] C. Bozzi,[27] R. Calabrese,[27] G. Cibinetto,[27] E. Luppi,[27] M. Negrini,[27] L. Piemontese,[27] F. Anulli,[28] R. Baldini-Ferroli,[28] A. Calcaterra,[28] R. de Sangro,[28] G. Finocchiaro,[28] S. Pacetti,[28] P. Patteri,[28] I. M. Peruzzi,[28,‡] M. Piccolo,[28] M. Rama,[28] A. Zallo,[28] A. Buzzo,[29] R. Capra,[29] R. Contri,[29] M. Lo Vetere,[29] M. M. Macri,[29] M. R. Monge,[29] S. Passaggio,[29] C. Patrignani,[29] E. Robutti,[29] A. Santroni,[29] S. Tosi,[29] G. Brandenburg,[30] K. S. Chaisanguanthum,[30] M. Morii,[30] J. Wu,[30] R. S. Dubitzky,[31] J. Marks,[31] S. Schenk,[31] U. Uwer,[31] W. Bhimji,[32] D. A. Bowerman,[32] P. D. Dauncey,[32] U. Egede,[32] R. L. Flack,[32] J. R. Gaillard,[32] J . A. Nash,[32] M. B. Nikolich,[32] W. Panduro Vazquez,[32] X. Chai,[33] M. J. Charles,[33] W. F. Mader,[33] U. Mallik,[33] V. Ziegler,[33] J. Cochran,[34] H. B. Crawley,[34] L. Dong,[34] V. Eyges,[34] W. T. Meyer,[34] S. Prell,[34] E. I. Rosenberg,[34] A. E. Rubin,[34] G. Schott,[35] N. Arnaud,[36] M. Davier,[36] G. Grosdidier,[36] A. Höcker,[36] F. Le Diberder,[36] V. Lepeltier,[36] A. M. Lutz,[36] A. Oyanguren,[36] T. C. Petersen,[36] S. Pruvot,[36] S. Rodier,[36] P. Roudeau,[36] M. H. Schune,[36] A. Stocchi,[36] W. F. Wang,[36] G. Wormser,[36] C. H. Cheng,[37] D. J. Lange,[37] D. M. Wright,[37] C. A. Chavez,[38] I. J. Forster,[38] J. R. Fry,[38] E. Gabathuler,[38] R. Gamet,[38] K. A. George,[38] D. E. Hutchcroft,[38] D. J. Payne,[38] K. C. Schofield,[38] C. Touramanis,[38] A. J. Bevan,[39] F. Di Lodovico,[39] W. Menges,[39] R. Sacco,[39] C. L. Brown,[40] G. Cowan,[40] H. U. Flaecher,[40] D. A. Hopkins,[40] P. S. Jackson,[40] T. R. McMahon,[40] S. Ricciardi,[40] F. Salvatore,[40] D. N. Brown,[41] C. L. Davis,[41] J. Allison,[42] N. R. Barlow,[42] R. J. Barlow,[42] Y. M. Chia,[42] C. L. Edgar,[42] M. P. Kelly,[42] G. D. Lafferty,[42] M. T. Naisbit,[42] J. C. Williams,[42] J. I. Yi,[42] C. Chen,[43] W. D. Hulsbergen,[43] A. Jawahery,[43] D. Kovalskyi,[43] C. K. Lae,[43] D. A. Roberts,[43] G. Simi,[43] G. Blaylock,[44] C. Dallapiccola,[44] S. S. Hertzbach,[44] X. Li,[44] T. B. Moore,[44] S. Saremi,[44] H. Staengle,[44] S. Y. Willocq,[44] R. Cowan,[45] K. Koeneke,[45] G. Sciolla,[45] S. J. Sekula,[45] M. Spitznagel,[45] F. Taylor,[45] R. K. Yamamoto,[45] H. Kim,[46] P. M. Patel,[46] C. T. Potter,[46] S. H. Robertson,[46] A. Lazzaro,[47] V. Lombardo,[47] F. Palombo,[47] J. M. Bauer,[48] L. Cremaldi,[48] V. Eschenburg,[48] R. Godang,[48] R. Kroeger,[48] J. Reidy,[48] D. A. Sanders,[48] D. J. Summers,[48] H. W. Zhao,[48] S. Brunet,[49] D. Côté,[49] M. Simard,[49] P. Taras,[49] F. B. Viaud,[49] H. Nicholson,[50] N. Cavallo,[51,§] G. De Nardo,[51] F. Fabozzi,[51,§] C. Gatto,[51] L. Lista,[51] D. Monorchio,[51] P. Paolucci,[51] D. Piccolo,[51] C. Sciacca,[51] M. Baak,[52] H. Bulten,[52] G. Raven,[52] H. L. Snoek,[52] C. P. Jessop,[53] J. M. LoSecco,[53] T. Allmendinger,[54] G. Benelli,[54] K. K. Gan,[54] K. Honscheid,[54] D. Hufnagel,[54] P. D. Jackson,[54] H. Kagan,[54] R. Kass,[54] T. Pulliam,[54] A. M. Rahimi,[54] R. Ter-Antonyan,[54] Q. K. Wong,[54] N. L. Blount,[55] J. Brau,[55] R. Frey,[55] O. Igonkina,[55] M. Lu,[55] R. Rahmat,[55] N. B. Sinev,[55] D. Strom,[55] J. Strube,[55] E. Torrence,[55] F. Galeazzi,[56] A. Gaz,[56] M. Margoni,[56] M. Morandin,[56] A. Pompili,[56] M. Posocco,[56] M. Rotondo,[56]

F. Simonetto,[56] R. Stroili,[56] C. Voci,[56] M. Benayoun,[57] J. Chauveau,[57] P. David,[57] L. Del Buono,[57] Ch. de la Vaissière,[57] O. Hamon,[57] B. L. Hartfiel,[57] M. J. J. John,[57] Ph. Leruste,[57] J. Malclès,[57] J. Ocariz,[57] L. Roos,[57] G. Therin,[57] P. K. Behera,[58] L. Gladney,[58] J. Panetta,[58] M. Biasini,[59] R. Covarelli,[59] M. Pioppi,[59] C. Angelini,[60] G. Batignani,[60] S. Bettarini,[60] F. Bucci,[60] G. Calderini,[60] M. Carpinelli,[60] R. Cenci,[60] F. Forti,[60] M. A. Giorgi,[60] A. Lusiani,[60] G. Marchiori,[60] M. A. Mazur,[60] M. Morganti,[60] N. Neri,[60] E. Paoloni,[60] G. Rizzo,[60] J. Walsh,[60] M. Haire,[61] D. Judd,[61] D. E. Wagoner,[61] J. Biesiada,[62] N. Danielson,[62] P. Elmer,[62] Y. P. Lau,[62] C. Lu,[62] J. Olsen,[62] A. J. S. Smith,[62] A. V. Telnov,[62] F. Bellini,[63] G. Cavoto,[63] A. D'Orazio,[63] E. Di Marco,[63] R. Faccini,[63] F. Ferrarotto,[63] F. Ferroni,[63] M. Gaspero,[63] L. Li Gioi,[63] M. A. Mazzoni,[63] S. Morganti,[63] G. Piredda,[63] F. Polci,[63] F. Safai Tehrani,[63] C. Voena,[63] H. Schröder,[64] R. Waldi,[64] T. Adye,[65] N. De Groot,[65] B. Franek,[65] E. O. Olaiya,[65] F. F. Wilson,[65] S. Emery,[66] A. Gaidot,[66] S. F. Ganzhur,[66] G. Hamel de Monchenault,[66] W. Kozanecki,[66] M. Legendre,[66] B. Mayer,[66] G. Vasseur,[66] Ch. Yèche,[66] M. Zito,[66] W. Park,[67] M. V. Purohit,[67] A. W. Weidemann,[67] J. R. Wilson,[67] M. T. Allen,[68] D. Aston,[68] R. Bartoldus,[68] P. Bechtle,[68] N. Berger,[68] A. M. Boyarski,[68] R. Claus,[68] J. P. Coleman,[68] M. R. Convery,[68] M. Cristinziani,[68] J. C. Dingfelder,[68] D. Dong,[68] J. Dorfan,[68] D. Dujmic,[68] W. Dunwoodie,[68] R. C. Field,[68] T. Glanzman,[68] S. J. Gowdy,[68] V. Halyo,[68] C. Hast,[68] T. Hryn'ova,[68] W. R. Innes,[68] M. H. Kelsey,[68] P. Kim,[68] M. L. Kocian,[68] D. W. G. S. Leith,[68] J. Libby,[68] S. Luitz,[68] V. Luth,[68] H. L. Lynch,[68] D. B. MacFarlane,[68] H. Marsiske,[68] R. Messner,[68] D. R. Muller,[68] C. P. O'Grady,[68] V. E. Ozcan,[68] A. Perazzo,[68] M. Perl,[68] B. N. Ratcliff,[68] A. Roodman,[68] A. A. Salnikov,[68] R. H. Schindler,[68] J. Schwiening,[68] A. Snyder,[68] J. Stelzer,[68] D. Su,[68] M. K. Sullivan,[68] K. Suzuki,[68] S. K. Swain,[68] J. M. Thompson,[68] J. Va'vra,[68] N. van Bakel,[68] M. Weaver,[68] A. J. R. Weinstein,[68] W. J. Wisniewski,[68] M. Wittgen,[68] D. H. Wright,[68] A. K. Yarritu,[68] K. Yi,[68] C. C. Young,[68] P. R. Burchat,[69] A. J. Edwards,[69] S. A. Majewski,[69] B. A. Petersen,[69] C. Roat,[69] L. Wilden,[69] S. Ahmed,[70] M. S. Alam,[70] R. Bula,[70] J. A. Ernst,[70] V. Jain,[70] B. Pan,[70] M. A. Saeed,[70] F. R. Wappler,[70] S. B. Zain,[70] W. Bugg,[71] M. Krishnamurthy,[71] S. M. Spanier,[71] R. Eckmann,[72] J. L. Ritchie,[72] A. Satpathy,[72] R. F. Schwitters,[72] J. M. Izen,[73] I. Kitayama,[73] X. C. Lou,[73] S. Ye,[73] F. Bianchi,[74] M. Bona,[74] F. Gallo,[74] D. Gamba,[74] M. Bomben,[75] L. Bosisio,[75] C. Cartaro,[75] F. Cossutti,[75] G. Della Ricca,[75] S. Dittongo,[75] S. Grancagnolo,[75] L. Lanceri,[75] L. Vitale,[75] V. Azzolini,[76] F. Martinez-Vidal,[76] R. S. Panvini,[77,||] Sw. Banerjee,[78] B. Bhuyan,[78] C. M. Brown,[78] D. Fortin,[78] K. Hamano,[78] R. Kowalewski,[78] I. M. Nugent,[78] J. M. Roney,[78] R. J. Sobie,[78] J. J. Back,[79] P. F. Harrison,[79] T. E. Latham,[79] G. B. Mohanty,[79] H. R. Band,[80] X. Chen,[80] B. Cheng,[80] S. Dasu,[80] M. Datta,[80] A. M. Eichenbaum,[80] K. T. Flood,[80] M. T. Graham,[80] J. J. Hollar,[80] J. R. Johnson,[80] P. E. Kutter,[80] H. Li,[80] R. Liu,[80] B. Mellado,[80] A. Mihalyi,[80] A. K. Mohapatra,[80] Y. Pan,[80] M. Pierini,[80] R. Prepost,[80] P. Tan,[80] S. L. Wu,[80] Z. Yu,[80] and H. Neal[81]

[1]*Laboratoire de Physique des Particules, F-74941 Annecy-le-Vieux, France*
[2]*Universitat de Barcelona, Facultat de Fisica Dept. ECM, E-08028 Barcelona, Spain*
[3]*Università di Bari, Dipartimento di Fisica and INFN, I-70126 Bari, Italy*
[4]*Institute of High Energy Physics, Beijing 100039, China*
[5]*University of Bergen, Institute of Physics, N-5007 Bergen, Norway*
[6]*Lawrence Berkeley National Laboratory and University of California, Berkeley, California 94720, USA*
[7]*University of Birmingham, Birmingham, B15 2TT, United Kingdom*
[8]*Ruhr Universität Bochum, Institut für Experimentalphysik 1, D-44780 Bochum, Germany*
[9]*University of Bristol, Bristol BS8 1TL, United Kingdom*
[10]*University of British Columbia, Vancouver, British Columbia, Canada V6T 1Z1*
[11]*Brunel University, Uxbridge, Middlesex UB8 3PH, United Kingdom*
[12]*Budker Institute of Nuclear Physics, Novosibirsk 630090, Russia*
[13]*University of California at Irvine, Irvine, California 92697, USA*
[14]*University of California at Los Angeles, Los Angeles, California 90024, USA*
[15]*University of California at Riverside, Riverside, California 92521, USA*
[16]*University of California at San Diego, La Jolla, California 92093, USA*
[17]*University of California at Santa Barbara, Santa Barbara, California 93106, USA*
[18]*University of California at Santa Cruz, Institute for Particle Physics, Santa Cruz, California 95064, USA*
[19]*California Institute of Technology, Pasadena, California 91125, USA*
[20]*University of Cincinnati, Cincinnati, Ohio 45221, USA*
[21]*University of Colorado, Boulder, Colorado 80309, USA*
[22]*Colorado State University, Fort Collins, Colorado 80523, USA*
[23]*Universität Dortmund, Institut für Physik, D-44221 Dortmund, Germany*
[24]*Technische Universität Dresden, Institut für Kern- und Teilchenphysik, D-01062 Dresden, Germany*
[25]*Ecole Polytechnique, LLR, F-91128 Palaiseau, France*
[26]*University of Edinburgh, Edinburgh EH9 3JZ, United Kingdom*
[27]*Università di Ferrara, Dipartimento di Fisica and INFN, I-44100 Ferrara, Italy*

[28]Laboratori Nazionali di Frascati dell'INFN, I-00044 Frascati, Italy

[29]Università di Genova, Dipartimento di Fisica and INFN, I-16146 Genova, Italy

[30]Harvard University, Cambridge, Massachusetts 02138, USA

[31]Universität Heidelberg, Physikalisches Institut, Philosophenweg 12, D-69120 Heidelberg, Germany

[32]Imperial College London, London, SW7 2AZ, United Kingdom

[33]University of Iowa, Iowa City, Iowa 52242, USA

[34]Iowa State University, Ames, Iowa 50011-3160, USA

[35]Universität Karlsruhe, Institut für Experimentelle Kernphysik, D-76021 Karlsruhe, Germany

[36]Laboratoire de l'Accélérateur Linéaire, IN2P3-CNRS et Université Paris-Sud 11, Centre Scientifique d'Orsay, B.P. 34, F-91898 ORSAY Cedex, France

[37]Lawrence Livermore National Laboratory, Livermore, California 94550, USA

[38]University of Liverpool, Liverpool L69 7ZE, United Kingdom

[39]Queen Mary, University of London, E1 4NS, United Kingdom

[40]University of London, Royal Holloway and Bedford New College, Egham, Surrey TW20 0EX, United Kingdom

[41]University of Louisville, Louisville, Kentucky 40292, USA

[42]University of Manchester, Manchester M13 9PL, United Kingdom

[43]University of Maryland, College Park, Maryland 20742, USA

[44]University of Massachusetts, Amherst, Massachusetts 01003, USA

[45]Massachusetts Institute of Technology, Laboratory for Nuclear Science, Cambridge, Massachusetts 02139, USA

[46]McGill University, Montréal, Québec, Canada H3A 2T8

[47]Università di Milano, Dipartimento di Fisica and INFN, I-20133 Milano, Italy

[48]University of Mississippi, University, Mississippi 38677, USA

[49]Université de Montréal, Physique des Particules, Montréal, Québec, Canada H3C 3J7

[50]Mount Holyoke College, South Hadley, Massachusetts 01075, USA

[51]Università di Napoli Federico II, Dipartimento di Scienze Fisiche and INFN, I-80126, Napoli, Italy

[52]NIKHEF, National Institute for Nuclear Physics and High Energy Physics, NL-1009 DB Amsterdam, The Netherlands

[53]University of Notre Dame, Notre Dame, Indiana 46556, USA

[54]Ohio State University, Columbus, Ohio 43210, USA

[55]University of Oregon, Eugene, Oregon 97403, USA

[56]Università di Padova, Dipartimento di Fisica and INFN, I-35131 Padova, Italy

[57]Universités Paris VI et VII, Laboratoire de Physique Nucléaire et de Hautes Energies, F-75252 Paris, France

[58]University of Pennsylvania, Philadelphia, Pennsylvania 19104, USA

[59]Università di Perugia, Dipartimento di Fisica and INFN, I-06100 Perugia, Italy

[60]Università di Pisa, Dipartimento di Fisica, Scuola Normale Superiore and INFN, I-56127 Pisa, Italy

[61]Prairie View A&M University, Prairie View, Texas 77446, USA

[62]Princeton University, Princeton, New Jersey 08544, USA

[63]Università di Roma La Sapienza, Dipartimento di Fisica and INFN, I-00185 Roma, Italy

[64]Universität Rostock, D-18051 Rostock, Germany

[65]Rutherford Appleton Laboratory, Chilton, Didcot, Oxon, OX11 0QX, United Kingdom

[66]DSM/Dapnia, CEA/Saclay, F-91191 Gif-sur-Yvette, France

[67]University of South Carolina, Columbia, South Carolina 29208, USA

[68]Stanford Linear Accelerator Center, Stanford, California 94309, USA

[69]Stanford University, Stanford, California 94305-4060, USA

[70]State University of New York, Albany, New York 12222, USA

[71]University of Tennessee, Knoxville, Tennessee 37996, USA

[72]University of Texas at Austin, Austin, Texas 78712, USA

[73]University of Texas at Dallas, Richardson, Texas 75083, USA

[74]Università di Torino, Dipartimento di Fisica Sperimentale and INFN, I-10125 Torino, Italy

[75]Università di Trieste, Dipartimento di Fisica and INFN, I-34127 Trieste, Italy

[76]IFIC, Universitat de Valencia-CSIC, E-46071 Valencia, Spain

[77]Vanderbilt University, Nashville, Tennessee 37235, USA

[78]University of Victoria, Victoria, British Columbia, Canada V8W 3P6

[79]Department of Physics, University of Warwick, Coventry CV4 7AL, United Kingdom

[80]University of Wisconsin, Madison, Wisconsin 53706, USA

---

[*]Also with the Johns Hopkins University, Baltimore, MD 21218, USA

[†]Also at Laboratoire de Physique Corpusculaire, Clermont-Ferrand, France

[‡]Also with Università di Perugia, Dipartimento di Fisica, Perugia, Italy

[§]Also with Università della Basilicata, Potenza, Italy

[‖]Deceased

^{81}*Yale University, New Haven, Connecticut 06511, USA*

From a sample of 232×10^6 $Y(4S) \rightarrow B\overline{B}$ events collected with the *BABAR* detector at the PEP-II *B* Factory in 1999–2004, we measure the $B^- \rightarrow D^0 K^{*-}(892)$ decay branching fraction using events where the K^{*-} is reconstructed in the $K_S^0 \pi^-$ mode and the D^0 in the $K^- \pi^+$, $K^- \pi^+ \pi^0$, and $K^- \pi^+ \pi^+ \pi^-$ channels: $\mathcal{B}(B^- \rightarrow D^0 K^{*-}(892)) = (5.29 \pm 0.30(\text{stat}) \pm 0.34(\text{syst})) \times 10^{-4}$.

The decays $B^- \rightarrow D^0 K^{(*)-}$ [1] are of interest because of their relevance to the Cabibbo-Kobayashi-Maskawa (CKM) model [2] of quark-flavor mixing. Interference effects in specific D^0 final states offer a means of observing direct CP violation governed by the angle $\gamma = \arg(-V_{ud}V_{ub}^*/V_{cd}V_{cb}^*)$ [3], where V is the CKM matrix. One way to access γ is to measure $\mathcal{R}_{CP\pm}$ [4]:

$$\mathcal{R}_{CP\pm} = 2\frac{\Gamma(B^- \rightarrow D_{CP\pm}^0 K^{*-}) + \Gamma(B^+ \rightarrow D_{CP\pm}^0 K^{*+})}{\Gamma(B^- \rightarrow D^0 K^{*-}) + \Gamma(B^+ \rightarrow \bar{D}^0 K^{*+})}.$$

Neglecting $D^0 - \bar{D}^0$ mixing $\mathcal{R}_{CP\pm}$ can be expressed in terms of a CP-conserving strong phase difference (δ), the ratio of the magnitude of suppressed and favored amplitudes (r_B), and γ: $\mathcal{R}_{CP\pm} = 1 \pm 2r_B \cos\delta \cos\gamma + r_B^2$. Thus a precise determination of the $B^- \rightarrow D^0 K^{*-}$ branching fraction provides the reference for direct CP violation measurements.

The decay $B^- \rightarrow D^0 K^{*-}$ was first observed by CLEO [5], and later by *BABAR* [6]. In this paper we present a new measurement of the branching fraction $\mathcal{B}(B^- \rightarrow D^0 K^{*-})$ obtained with 2.7 times more data than used for the previous *BABAR* measurement.

This analysis uses data collected with the *BABAR* detector at the PEP-II $e^+ e^-$ storage ring. The data corresponds to an integrated luminosity of 211 fb^{-1} at the $Y(4S)$ peak (232×10^6 $B\overline{B}$ pairs) and 16 fb^{-1} at center-of-mass energy 40 MeV below the resonance.

The *BABAR* detector is described in detail in [7]. We give here a brief description of the components relevant to this analysis. Charged-particle trajectories are measured by a five-layer double-sided silicon vertex tracker (SVT) and a 40-layer drift chamber (DCH) inside a 1.5 T solenoid. Charged-particle identification is achieved by combining measurements of the light detected in a ring-imaging Cherenkov device (DIRC) with measurements of the ionization energy loss (dE/dx) measured in the DCH and SVT. Photons are detected in a CsI(Tl) electromagnetic calorimeter (EMC) inside the coil. We use GEANT4 [8] based software to simulate the detector response and account for the varying beam and environmental conditions.

To reconstruct $B^- \rightarrow D^0 K^{*-}$ decays we select K^{*-} candidates in the $K^{*-} \rightarrow K_S^0 \pi^-$ mode and D^0 candidates in three decay channels: $D^0 \rightarrow K^- \pi^+$, $K^- \pi^+ \pi^0$, and $K^- \pi^+ \pi^+ \pi^-$. Our event selection follows closely the one reported in [9]. K_S^0 candidates are formed from oppo-

sitely charged tracks assumed to be pions with a reconstructed invariant mass within 13 MeV/c^2 (4 standard deviations) of the known K_S^0 mass, $m_{K_S^0}$ [10]. The K_S^0 candidates are fitted so that their invariant mass equals $m_{K_S^0}$ (mass constraint). We further require their flight direction and distance to be consistent with a K_S^0 coming from the interaction point. The K_S^0 candidate's flight path and momentum vectors must make an acute angle and the flight length in the plane transverse to the beam must be at least 3 times larger than its uncertainty. K^{*-} candidates are formed from a K_S^0 and a charged particle, which are required to originate from a common vertex. We select K^{*-} candidates which have an invariant mass within 75 MeV/c^2 of the known value [10]. Finally, since the K^{*-} in $B^- \rightarrow D^0 K^{*-}$ is polarized, we require the helicity angle θ_H to satisfy $|\cos\theta_H| \gtrsim 0.35$, where θ_H is the angle in the K^{*-} rest frame between the daughter pion and the parent B momentum. The helicity distribution discriminates well between a B meson decay and an event from the $e^+ e^- \rightarrow q\bar{q}(q \in \{u, d, s, c\})$ continuum, since the former is distributed as $\cos^2\theta_H$ and the latter is almost flat.

In order to reconstruct the π^0 of the $D^0 \rightarrow K^- \pi^+ \pi^0$ channel, we combine pairs of photons to form candidates with a total energy greater than 200 MeV and an invariant mass between 125 and 145 MeV/c^2. A mass-constrained fit is applied to the selected π^0 candidates. All D^0 candidates are mass- and vertex-constrained. Particle identification is required for the charged kaons. We select D^0 candidates with an unconstrained invariant mass, m_{D^0}, differing from the world average mass, $m_{D^0}^{\text{PDG}}$, by less than 12 MeV/c^2 for all channels except $K^- \pi^+ \pi^0$ where we require $-29 < m_{D^0} - m_{D^0}^{\text{PDG}} < +24$ MeV/c^2. To reduce combinatorial background in this channel, we further select candidates in the regions of the Dalitz plane enhanced by the $K^{*-}(892)$, $K^{*0}(892)$ and $\rho^+(770)$ resonances using amplitudes and phases measured by the CLEO experiment [11]. In order to reduce the background from random two track combinations that have masses consistent with a D^0 we also require, for the $D^0 \rightarrow K^- \pi^+$ channel, $|\cos\theta_D| \leq 0.9$, where θ_D is the angle in the D^0 rest frame between the daughter kaon and the parent B momentum. Finally, we perform a geometric fit on the B candidate which constrains the D^0, the K_S^0, and the charged pion from the K^{*-} to originate from a single vertex.

To suppress continuum background we require $|\cos\theta_B^*| \leq 0.9$, where θ_B^* is defined as the angle between

the B candidate momentum in the $Y(4S)$ rest frame and the beam axis. The distribution in $\cos\theta_B^*$ is flat for $q\bar{q}$ events, while for B mesons it follows a $\sin^2\theta_B^*$ distribution. We also use global event shape variables to distinguish between $q\bar{q}$ continuum events which have a two-jet topology in the $Y(4S)$ rest frame and $B\bar{B}$ events which are more spherical. We require $|\cos\theta_T^*| \le 0.9$ where θ_T^* is the angle between the thrust axes of the B candidate and that of the rest of the event. We construct a linear (Fisher) discriminant [12] from $\cos\theta_T^*$ and the L_0, L_2 monomials (see below) describing the energy flow in the rest of the event, as in [13]. In the center-of-mass frame (CM) we define $L_j = \Sigma_i p_i^* |\cos\theta_i^*|^j$, where i indexes the charged and neutral particles in the event once those from the B candidate are removed, and θ_i^* is the angle of the CM-momentum p_i^* with the thrust axis of the B meson candidate.

We identify B candidates using two nearly independent kinematic variables: the beam-energy-substituted mass $m_{ES} = \sqrt{(s/2 + \mathbf{p_0} \cdot \mathbf{p_B})^2/E_0^2 - p_B^2}$ and the energy difference $\Delta E = E_B^* - \sqrt{s}/2$, where E and p are energy and momentum, the subscripts 0 and B refer to the e^+e^--beam-system and the B candidate in the lab frame, respectively; s is the square of the CM energy, and the asterisk labels the CM frame.

In those events where we find more than one acceptable B candidate (less than 25% of selected events depending on the D^0 mode), we choose the one with the smallest χ^2 formed from the differences of the measured and world average D^0 and K^{*-} masses scaled by the mass resolution which includes the experimental resolution and, for the K^{*-}, its natural width. Simulations show that no bias is introduced by this choice and the correct candidate is picked at least 80% of the time. According to simulation of signal events, the total reconstruction efficiencies are: 13.3%, 4.6%, and 9.0% for the $D^0 \to K^-\pi^+$, $K^-\pi^+\pi^0$, and $K^-\pi^+\pi^+\pi^-$ modes, respectively.

To study $B\bar{B}$ backgrounds we look at sideband regions away from the signal region in ΔE and m_{D^0}. The ΔE distributions are centered around zero for signal with a resolution between 11 and 13 MeV for all three channels. We define a signal region $|\Delta E| < 25$ MeV. We also define a ΔE sideband in the intervals $-100 \le \Delta E \le -60$ MeV and $60 \le \Delta E \le 200$ MeV. The lower limit (-100 MeV) is chosen to avoid selecting a region of high background coming from $B^- \to D^*K^{*-}$. In this ΔE sideband we see no significant evidence of a background peaking near the B mass in m_{ES} which could leak into the signal region. The sideband region in m_{D^0} is defined by requiring that this quantity differs from the D^0 mass peak by more than 4 standard deviations. It provides sensitivity to doubly-peaking background sources that mimic signal both in ΔE and m_{ES}. This pollution comes from either charmed or charmless B meson decays that do not contain a true D^0. Since many of the possible contributions to this background are not well known, we attempt to measure its

size by including the m_{D^0} sideband in the fit described below.

An unbinned extended maximum likelihood fit to m_{ES} distributions in the range $5.2 \le m_{ES} \le 5.3$ GeV/c^2 is used to determine the event yields. For signal modes, the m_{ES} distributions are described by a Gaussian function $\mathcal{G}$ centered at the B mass with resolution (σ), averaged over the three D^0 decay modes, of 2.7 MeV/c^2. For each D^0 decay mode $k(= 1, 2, 3)$ we determine the mean and sigma of the Gaussian $\mathcal{G}_k$ by fitting to the data. The combinatorial background in the m_{ES} distribution is modeled with a threshold function $\mathcal{A}_k$ [14]. Its shape is governed by one parameter ξ_k that is left free in the fit for each D^0 decay mode. We fit simultaneously m_{ES} distributions of nine samples: the $K^-\pi^+$, the $K^-\pi^+\pi^0$ and $K^-\pi^+\pi^-\pi^+$ samples for (i) the ΔE signal region, (ii) the m_{D^0} sideband and (iii) the ΔE sideband. We fit three probability density functions (PDF) weighted by the unknown event yields. For the ΔE sideband, we use $\mathcal{A}_k$. For the m_{D^0} sideband we use $N_{noP}^k \cdot \mathcal{A}_k + N_{DP}^k \cdot \mathcal{G}_k$, where $\mathcal{G}_k$ accounts for the doubly-peaking B decays. For the signal region PDF we use $N_{q\bar{q}}^k \cdot \mathcal{A}_k + \kappa N_{DP}^k \cdot \mathcal{G}_k + N_{sig}^k \cdot \mathcal{G}_k$, where κ is the ratio of the m_{D^0} signal-window to sideband widths and N_{sig}^k is the number of $B^- \to D^0 K^{*-}$ signal events. The ΔE sideband sample helps define the shape of the background function $\mathcal{A}_k$. We assume that the B decays found in the
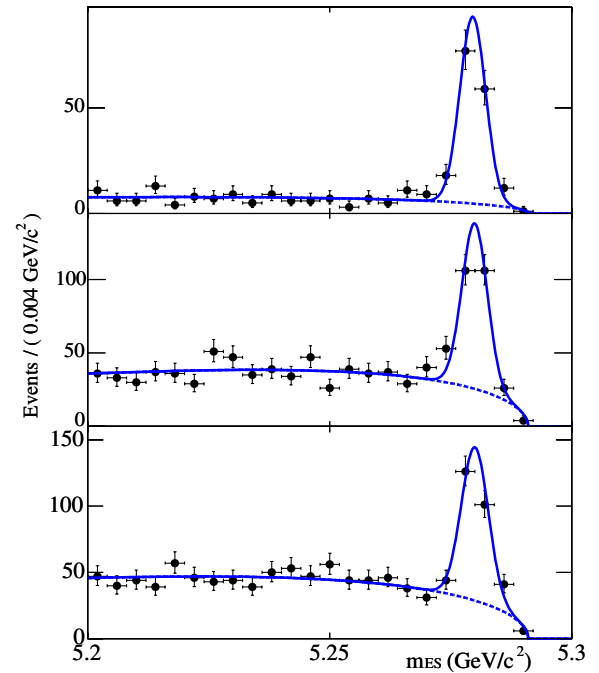

FIG. 1 (color online). Distributions of m_{ES} in the signal region for $B^- \to D^0 K^{*-}$ decays where $D^0 \to K^-\pi^+$ (top), $K^-\pi^+\pi^0$ (middle), and $K^-\pi^+\pi^-\pi^+$ (bottom). The dashed curve indicates the contribution from the combinatorial background and the peaking B-background which is estimated from a simultaneous fit to the D^0 sideband (not shown).

TABLE I.   Results from the fit and quantities used to derive the $B^- \to D^0 K^{*-}$ branching fraction. For each channel we give the event yield resulting from the fit, the efficiency, and the branching fraction measurement, in units of 10^{-4}, derived using Eq. (1). The uncertainties are statistical only.

	$K^- \pi^+$	$K^- \pi^+ \pi^0$	$K^- \pi^+ \pi^- \pi^+$
Yield	144 ± 13	185 ± 19	195 ± 18
Efficiency	13.30%	4.60%	8.99%
$\mathcal{B}(B^- \to D^0 K^{*-})$	5.15 ± 0.47	5.65 ± 0.57	5.24 ± 0.49

m_{D^0} sideband have the same final states as the signal so we use the same Gaussian shape for the doubly-peaking B background.

The fit results are shown graphically in Fig. 1 and numerically in Table I. For each channel k, a measurement $\mathcal{B}_k$ of the branching fraction $\mathcal{B}(B^- \to D^0 K^{*-})$ is derived as follows:

$$\mathcal{B}_k = \frac{N(D^0 \to X_k) \cdot f}{N_{B^\pm} \cdot \varepsilon_k \cdot \mathcal{B}_{K^{*-}} \cdot \mathcal{B}(D^0 \to X_k)}, \qquad (1)$$

where $N(D^0 \to X_k)$ is the event yield from the fit, f the fraction of K^{*-}'s in the sample (discussed below), $N_{B^\pm}$ is the number of charged B mesons in the data sample, ε_k is the efficiency to reconstruct $B^- \to D^0 K^{*-}$ when $D^0 \to X_k$, $\mathcal{B}_{K^{*-}} \equiv \mathcal{B}(K^{*-} \to K_S^0 \pi) \cdot \mathcal{B}(K_S^0 \to \pi^+ \pi^-)$ and $\mathcal{B}(D^0 \to X_k)$ are the branching fractions of the K^{*-} and the D^0. We have assumed equal production of pairs of neutral and charged B mesons in $Y(4S)$ decay.

Systematic effects arise from the difference between the actual detector response for the data and the simulation model for the Monte Carlo. Here the main effects stem from the modeling of the tracking efficiency (1.2–1.3% per track), the K_S^0 reconstruction efficiency (2% per K_S^0), the π^0 reconstruction efficiency for the $K^- \pi^+ \pi^0$ channel (3%) and the efficiency and misidentification probabilities from the particle identification (2% per kaon). A study of a high-statistics $B^- \to D^0 \pi^-$ control sample shows excellent agreement between the data and Monte Carlo sample except for the distributions of ΔE and the continuum-suppression Fisher discriminant. For these variables, differences of up to $(2.5 \pm 1.1)\%$ are measured between the data and Monte Carlo. Suitable corrections to the efficiencies are therefore applied and systematic errors assigned. The K^{*-} helicity angle distributions differ significantly between data and simulation because of the nonresonant background under the K^{*-} peak. We describe below how we subtract this background. For the pure K^{*-} events, we estimate that the residual discrepancy between data and simulation in the helicity to be less than 1.6%. We determine using simulations that the m_{ES} signal PDFs deviate from the single Gaussian shape by less than 0.1%. Substantial systematic uncertainties come from the measured D^0 branching fractions [10] and the number of $B^\pm$ pairs in the sample.
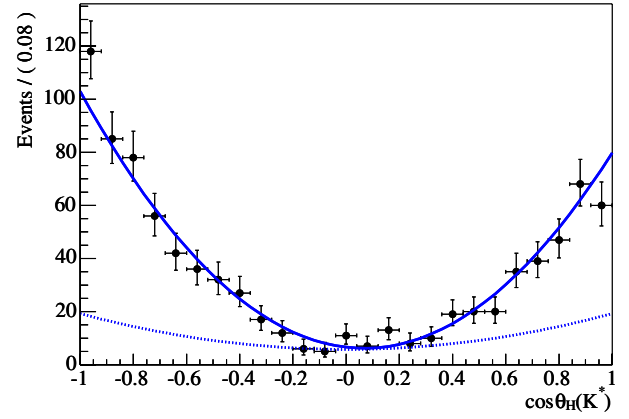

FIG. 2 (color online).   Acceptance corrected distribution of $\cos\theta_H(K^{*-})$. The solid line is a fit to a model which includes *P*-wave and *S*-wave interference as well as combinatorial background. The dotted line shows the combinatorial background estimated from the data.

The observed number of signal events must be corrected for the nonresonant $K_S^0 \pi$ pairs under the K^{*-}. When we remove the requirement on the K^{*-} helicity angle, we see that the K^{*-} helicity distribution (Fig. 2) of the selected events manifests a forward-backward asymmetry that indicates an interference with a $K_S^0 \pi$ background [9,15]. We model the $K_S^0 \pi^-$ system with a *P*-wave and an *S*-wave component. The *P*-wave mass dependence is described by a relativistic Breit-Wigner while the *S*-wave piece is assumed to be a complex constant. This model is fitted to the data and shown in Fig. 2 along with an estimate of the combinatorial background. Neglecting higher resonances, the number of $K_S^0 \pi^-$ peaking background events is $(4 \pm 1)\%$ of the total measured number of signal events. We do not quote a systematic error on the contributions of the neglected partial waves (non-K^* *P*-wave and higher order waves) since their expected rates in the $K\pi$ mass window are far below that of the *S*-wave [15]. In Fig. 3 we see that a
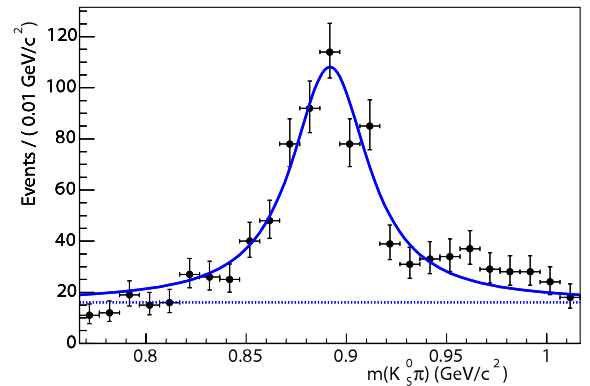

FIG. 3 (color online).   Invariant mass of $K_s^0 \pi^-$ combinations with all other analysis cuts applied. The solid curve is a Breit-Wigner line shape including detector resolution. The dotted line shows the combinatorial background.

TABLE II. Systematic uncertainties. X_k refers to the D^0 decay modes given in the columns. $\mathcal{B}_{K^{*-}}$ is the branching fraction of the $K^{*-} \to K_S^0 \pi^-$, $K_S^0 \to \pi^+ \pi^-$ decay chain.

Source	$K^- \pi^+$	$K^- \pi^+ \pi^0$	$K^- \pi^+ \pi^- \pi^+$
Tracking efficiency	3.8%	3.8%	6.3%
π^0 efficiency	-	3.1%	-
Particle Identification	2.0%	2.0%	2.0%
K_S^0 efficiency	1.6%	1.9%	1.8%
$\cos\theta_H(K^{*-})$	1.6%	1.6%	1.6%
Fisher	1.1%	1.1%	1.1%
ΔE	1.9%	1.8%	2.0%
m_{ES} PDF shape	0.1%	0.1%	0.1%
Number of $B^\pm$	1.1%	1.1%	1.1%
Simulation statistics	0.9%	1.4%	1.0%
$\mathcal{B}_{K^{*-}}$ [10]	0.2%	0.2%	0.2%
$\mathcal{B}(D^0 \to X_k)$ [10]	2.4%	6.2%	4.2%
$K_S^0 \pi^-$ S-wave subtraction	1.1%	1.1%	1.1%
Total systematic error	6.1%	9.0%	8.7%

relativistic Breit-Wigner gives a fair description of the resonance structure in the $K_S^0 \pi^-$ mass spectrum ($\chi^2 = 26.8$ for 20 degrees of freedom).

All sources of systematic uncertainties are listed for each mode in Table II. With the exception of ΔE and simulation statistics the systematic error sources listed in Table II are correlated among the different D^0 modes. We use the procedure discussed in [16] to form a weighted average of the three D^0 decay modes and determine:

$$\mathcal{B}(B^- \to D^0 K^{*-}) = (5.29 \pm 0.30 \pm 0.34) \times 10^{-4}.$$

The first error is statistical and the second is systematic. We have compared the results from this analysis using the same data set as in our previously published analysis [6]. The two analyses use different selection criteria and therefore find different numbers of events. The results from the two analyses are consistent to within a half of a (statistical) standard deviation. We have also calculated the branching fraction for the two data sets obtained since the previous analysis. The measurement in each set is consistent with, although lower than the value obtained in [6]. This result supersedes our previously published result.

In summary, we have measured the branching fraction of the decay $B^- \to D^0 K^{*-}$ in the $D^0 K_S^0 \pi^-$ final state and observed the interference of the K^{*-} with a small non-resonant $K_S^0 \pi$ background.

[1] Reference to a charge conjugate mode is implied throughout the paper unless otherwise stated.

[2] N. Cabibbo, Phys. Rev. Lett. **10**, 531 (1963); M. Kobayashi and T. Maskawa, Prog. Theor. Phys. **49**, 652 (1973).

[3] M. Gronau and D. Wyler, Phys. Lett. B **265**, 172 (1991); I. Dunietz, Phys. Lett. B **270**, 75 (1991); D. Atwood, G. Eilam, M. Gronau, and A. Soni, Phys. Lett. B **341**, 372 (1995); D. Atwood, I. Dunietz, and A. Soni, Phys. Rev. Lett. **78**, 3257 (1997).

[4] M. Gronau, Phys. Rev. D **58**, 037301 (1998); Phys. Lett. B **557**, 198 (2003).

[5] R. Mahapatra *et al.* (CLEO Collaboration), Phys. Rev. Lett. **88**, 101803 (2002).

[6] B. Aubert *et al.* (*BABAR* Collaboration), Phys. Rev. D **69**, 051101 (2004).

[7] B. Aubert *et al.* (*BABAR* Collaboration), Nucl. Instrum. Methods Phys. Res., Sect. A **479**, 1 (2002).

[8] S. Agostinelli *et al.* (GEANT4 Collaboration), Nucl. Instrum. Methods Phys. Res., Sect. A **506**, 250 (2003).

[9] B. Aubert *et al.* (*BABAR* Collaboration), Phys. Rev. D **72**, 071103 (2005).

[10] S. Eidelman *et al.* (Particle Data Group), Phys. Lett. B **592**, 1 (2004).

[11] S. Kopp *et al.* (CLEO Collaboration), Phys. Rev. D **63**, 092001 (2001).

[12] R. A. Fisher, Annals Eugen. **7**, 179 (1936).

[13] B. Aubert *et al.* (*BABAR* Collaboration), Phys. Rev. Lett. **89**, 281802 (2002).

[14] H. Albrecht *et al.* (ARGUS collaboration), Phys. Lett. B **185**, 218 (1987); **241**, 278 (1990). The function is $\mathcal{A}(m_{ES}) \propto m_{ES}\sqrt{1 - x^2} \exp[-\xi(1 - x^2)]$, where $x = m_{ES}/E_{max}$ and ξ is a fit parameter.

[15] J. M. Link *et al.* (FOCUS collaboration), Phys. Lett. B **535**, 43 (2002); D. Aston *et al.* (LASS Collaboration), Nucl. Phys. **B296**, 493 (1988); E. M. Aitala *et al.* (E791 Collaboration), Phys. Rev. Lett. **89**, 121801 (2002).

[16] L. Lyons *et al.*, Nucl. Instrum. Methods Phys. Res., Sect. A **270**, 110 (1988).